

Original Article

Comparative Study of Chemosensory Organs of Shrimp From Hydrothermal Vent and Coastal Environments

Magali Zbinden¹, Camille Berthod¹, Nicolas Montagné², Julia Machon¹, Nelly Léger¹, Thomas Chertemps², Nicolas Rabet³, Bruce Shillito¹ and Juliette Ravaux¹

¹Sorbonne Universités, Univ Paris 06, UMR CNRS MNHN 7208 Biologie des Organismes Aquatiques et Ecosystèmes (BOREA), Equipe Adaptation aux Milieux Extrêmes, Bât. A, 4e étage, 7 Quai St Bernard, 75005 Paris, France, ²Sorbonne Universités, Univ Paris 06, Institut d'Ecologie et des Sciences de l'Environnement (iEES-Paris), 4 place Jussieu, 75005 Paris, France and ³Sorbonne Universités, Univ Paris 06, UMR CNRS MNHN 7208 Biologie des Organismes Aquatiques et Ecosystèmes (BOREA), Département des milieux et peuplements aquatiques, CP26, 43 rue Cuvier, 75005 Paris, France

Correspondence to be sent to: Magali Zbinden, Université Pierre et Marie Curie, UMR 7208 BOREA, 7 quai St Bernard - Bat A, 4ème étage, pièce 417 (Boîte 5), 75252 Paris Cedex 05, France. e-mail: magali.zbinden@upmc.fr

Editorial Decision 24 January 2017.

Abstract

The detection of chemical signals is involved in a variety of crustacean behaviors, such as social interactions, search and evaluation of food and navigation in the environment. At hydrothermal vents, endemic shrimp may use the chemical signature of vent fluids to locate active edifices, however little is known on their sensory perception in these remote deep-sea habitats. Here, we present the first comparative description of the sensilla on the antennules and antennae of 4 hydrothermal vent shrimp (*Rimicaris exoculata*, *Mirocaris fortunata*, *Chorocaris chacei*, and *Alvinocaris markensis*) and of a closely related coastal shrimp (*Palaemon elegans*). These observations revealed no specific adaptation regarding the size or number of aesthetascs (specialized unimodal olfactory sensilla) between hydrothermal and coastal species. We also identified partial sequences of the ionotropic receptor IR25a, a co-receptor putatively involved in olfaction, in 3 coastal and 4 hydrothermal shrimp species, and showed that it is mainly expressed in the lateral flagella of the antennules that bear the unimodal chemosensilla aesthetascs.

Key words: aesthetascs, decapod, hydrothermal shrimp, IR25a, olfaction

Introduction

Chemical senses are crucial in mediating important behavioral patterns for most animals. In crustaceans, chemical senses have been shown to play a role in various social interactions, search and evaluation of food, as well as in evaluation and navigation in the habitat (Stuellet et al. 2001; Derby and Weissburg 2014). Chemoreception in decapod crustaceans is mediated by chemosensory sensilla that are

mainly localized on the first antennae (antennules), pereopod dactyls and mouthparts (Ache 1982; Derby et al. 2016). Chemoreception has been proposed to be differentiated into 2 different modes (Schmidt and Mellon 2011; Mellon 2014; Derby et al. 2016): 1) “olfaction” mediated by olfactory receptor neurons (ORNs) housed in specialized unimodal olfactory sensilla (the aesthetascs), restricted to the lateral flagella of the antennules (Laverack 1964; Grünert and Ache 1988;

Cate and Derby 2001) and projecting to the olfactory lobe of the brain (Schmidt and Ache 1996b) and 2) “distributed chemoreception” mediated by numerous bimodal sensilla (containing mechano- and chemo-receptor neurons) occurring on all appendages, projecting to the second antenna and lateral antennular neuropils and the leg neuromeres (Schmidt and Ache 1996a). Although the molecular mechanisms of olfaction have been well studied in insects, they remain largely unknown in crustaceans, and the existing knowledge is restricted to a few number of model organisms (lobsters, crayfish, and the water flea *Daphnia pulex*; review in Derby et al. 2016). In particular, the nature of crustacean odorant receptors has remained elusive until recently, since searches for the traditional insect olfactory receptors have been unsuccessful. A new family of receptors involved in odorant detection, named the Ionotropic Receptors (IRs), was recently described in *Drosophila melanogaster*, and was subsequently shown to be conserved in Protostomia, including the crustacean *D. pulex* (Benton et al. 2009; review in Croset et al. 2010). Lately, several IRs were identified in other crustaceans, the spiny lobster *Panulirus argus* (Corey et al. 2013), the American lobster *Homarus americanus* (Hollins et al. 2003), the hermit crabs *Pagurus bernhardus* (Groh et al. 2014) and *Coenobita clypeatus* (Groh-Lunow et al. 2015), and were proposed to mediate the odorant detection in the antennules. In the lobster, the authors propose that IRs function as heteromeric receptors, with IR25a and IR93a being common subunits that associate with other IR subunits to determine the odor sensitivity of ORNs.

Chemoreception in crustaceans has been largely studied in large decapods like lobsters (Devine and Atema 1982; Cowan 1991; Moore et al. 1991; Derby et al. 2001; Shabani et al. 2008; and see review in Derby et al. 2016). However, this research theme remains poorly investigated in shrimp, especially in deep-sea species. Deep-sea hydrothermal vent shrimp inhabit patchy and ephemeral environments along the mid-oceanic ridges. Inhabiting such sparsely distributed habitats presents challenges for the detection of active emissions by endemic fauna, especially in the absence of light. In the early developmental stages, after release and dispersal in the water column, sometimes tens or hundreds of kilometers from their starting point, larvae need to locate a vent site to settle and begin their adult life (Pond et al. 1997; Herring and Dixon 1998). Later as adults, mobile vent fauna may need to evaluate their environment, to find hydrothermal fluid either to feed their symbiotic bacteria or just to be able to detect the appropriate habitat, in an environment characterized by steep physicochemical gradients (Sarradin et al. 1999; Sarrazin et al. 1999; Le Bris et al. 2006). Chemical compounds like sulfide, temperature and dim light emitted by vents have been proposed to be potential attractants for detection of hydrothermal emissions (Van Dover et al. 1989; Renninger et al. 1995; Gaten et al. 1998).

Only a few studies on olfaction in the hydrothermal shrimp *Rimicaris exoculata* have been published (Renninger et al. 1995; Chamberlain et al. 1996; Jinks et al. 1998), providing the first, brief, description of the sensilla on the antennules and antennae of this species. These authors also reported preliminary behavioral observations, suggesting an attraction to sulfide, and registered electrophysiological responses to sulfide in antennal filaments (but surprisingly not in the antennular lateral ones bearing aesthetascs).

Here, we present a comparative morphological description of antennae and antennules of 4 hydrothermal vent shrimp (*R. exoculata*, *Mirocaris fortunata*, *Chorocaris chacei*, and *Alvinocaris markensis*). We also identified partial sequences of the candidate co-receptor IR25a and studied its expression pattern in the different species. All the approaches were conducted in parallel on a

closely related coastal shrimp (*Palaemon elegans*), to give insights in the potential adaptations of sensory organs in deep-sea species. Comparisons within hydrothermal species were also conducted to examine possible specific adaptations related to their different environments and lifestyles, as previous studies showed that chemical senses of crustaceans rapidly evolve and present specialized adaptations according to phylogeny, lifestyle and habitat, as well as to trophic levels (Beltz et al. 2003; Derby and Weissburg 2014). Knowledge of the sensory capabilities of hydrothermal species is especially relevant with the growing interest of mining companies for extraction of seafloor massive sulfides hydrothermal deposits (Hoagland et al. 2010). Possible impacts of sulfide exploitation on vent species encompass habitat destruction, increase of suspended particles and the presence of higher levels of toxic elements, leading to physiological disturbances and to potential alteration of their ability to perceive their environment (Lahman and Moore 2015) and detect hydrothermal emissions.

Materials and methods

Choice of models

Shrimp are one of the dominant macrofaunal taxa of hydrothermal sites in the Mid-Atlantic Ridge (Desbruyères et al. 2000, 2001). They are highly motile, and according to species, occupy different habitats, exhibit different food diets, and show various degrees of association with bacteria. Therefore they provide good models for studying olfactory capabilities since individuals belonging to different species are potentially not sensitive to the same attractants. *Rimicaris exoculata* lives in dense swarms (up to 2500 ind/m², Desbruyères et al. 2001) on the chimney walls, at around 20–30 °C, near the fluid emissions in order to feed their dense symbiotic chemoautotrophic bacterial community (Van Dover et al. 1988; Zbinden et al. 2004, 2008). *Chorocaris chacei* is much less abundant (locally 2–3 ind/dm²) than *R. exoculata*, but may live close to it. It is also found as on sulfide blocks, in areas of weak fluid emissions (Desbruyères et al. 2006; Husson et al. 2016). *Chorocaris* also harbors a bacterial symbiotic community, though less developed than in *Rimicaris* (Segonzac 1992). *Mirocaris fortunata* lives at lower temperature (4.8–6.1 °C, Husson et al. 2016), in diffuse flow habitats and among *Bathymodiolus* mussel assemblages (Sarrazin et al. 2015). *Mirocaris* is opportunistic and feeds on mussel tissue, shrimp and other invertebrates, being reported as predators and/or scavengers (Gebruk et al. 2000; De Busserolles et al. 2009). *Alvinocaris markensis* occurs as solitary individuals, at the base of and on the walls of active edifices, close to *R. exoculata* aggregates, and also on mussel assemblages. It has been reported as necrophagous (Desbruyères et al. 2006), but also as a predator (Segonzac 1992).

In order to identify potential adaptations of hydrothermal shrimp sensory faculties, comparisons were made with the related shallow-water palaemonid species *P. elegans*. The description of palaemonid antennal structures is also interesting per se since olfaction is poorly analyzed in shrimp in general. Two additional palaemonid species, *Palaemon serratus* and *Palaemonetes varians*, were used for identifying the IR25a sequence.

Animal collection, conditioning, and maintenance

Specimens of Alvinocarididae *M. fortunata*, *R. exoculata*, *C. chacei*, and *A. markensis* were collected during the Momarsat 2011 and 2012, Biobaz 2013, and Bicose 2014 cruises, on the Mid-Atlantic Ridge (see Table 1 for cruises and sites). Shrimp were collected with the suction sampler of the ROV “Victor 6000” operating from the

RV “Pourquoi Pas?”. Immediately after retrieval, living specimens were dissected and tissues of interest (see below) were fixed in a 2.5% glutaraldehyde/seawater solution for morphological observations or frozen in liquid nitrogen for molecular biology experiments.

Specimens of Palaemonidae *P. elegans*, *P. serratus*, and *P. varians* were collected from Saint-Malo region (France; 48°64'N, -2°00'W), between October 2011 and January 2015, using a shrimp hand net. They were transported to the laboratory and transferred to aerated aquaria with a 12 h:12 h light:dark cycle, a salinity of 35 g/L, and a water temperature of 18 °C. The shrimp were regularly fed with granules (JBL Novo Prawn). Tissues of interest were also fixed in a 2.5% glutaraldehyde/seawater solution for morphological observations or frozen in liquid nitrogen for molecular biology experiments.

Tissue collection

For morphological observations, antennae and antennules (both medial and lateral flagella) were used. For molecular biology experiments, the following organs were dissected for *P. elegans*: the antennular medial and lateral flagella (internal and external ramus separated), the antennae, the mouthparts (mandibles and 2 pairs of maxillae), the first and second walking legs and the eyestalks. For the hydrothermal shrimp, the dissection included the following organs: the antennular medial and lateral flagella, the antennae, and abdominal muscles.

Scanning electron microscopy

Samples were post-fixed in osmium tetroxide 1% once in the lab and dehydrated through an ethanol series. They were then critical-point-dried (CPD7501, Quorum Technologies) and platinum-coated in a Scancoat six Edwards sputter-unit prior to observation in a scanning electron microscope (Cambridge Stereoscan 260), operating at 20 kV.

RNA extraction and reverse transcription

Frozen shrimp tissues were ground in TRIzol Reagent (Thermo Fisher Scientific) with a Minilys homogenizer (Bertin Corp). Total RNA was isolated according to the manufacturer's protocol, and quantified by spectrophotometry and electrophoresis in a 1.2% agarose gel under denaturing conditions. RNA (500 ng) was DNase treated to remove contamination using the TURBO DNase kit (Thermo Fisher Scientific) and then reverse transcribed to cDNA with the Superscript II reverse transcriptase kit (Thermo Fisher Scientific) using a oligo(dT)₁₈ primer according to the manufacturer's instructions.

IR25a sequencing and mRNA expression (reverse transcription polymerase chain reaction)

The cDNA fragments encoding IR25a were amplified by 2 rounds of polymerase chain reaction (PCR). Oligonucleotide primers were

designed from a multiple-sequence alignment of IR25a sequences of crustaceans (*D. pulex*, Croset et al. 2010; *H. americanus* AY098942, Hollins et al. 2003, *Lepeophtheirus salmonis* PRJNA280127 genome sequencing project), insects (*Acyrtosiphon pisum*, *Aedes aegypti*, *Anopheles gambiae*, *Apis mellifera*, *Bombyx mori*, *Culex quinquefasciatus*, *D. melanogaster*, *Nasonia vitripennis*, *Pediculus humanus*, *Tribolium castaneum*, Croset et al. 2010), gastropod molluscs (*Aphysia californica*, *Lottia gigantea*, Croset et al. 2010), nematods (*Caenorhabditis briggsae* XM_002643827, Stein et al. 2003, *Caenorhabditis elegans* NM_076040, The *C. elegans* Sequencing Consortium) and an annelid (*Capitella capitata*, Croset et al. 2010) (primer sequences are listed in Supplementary Table S1). PCR amplification reactions were performed in a 20 µL volume containing 1 µL of cDNA template, 2 µL of each primer [10 µM], 11.7 µL of H₂O, 2 µL of PCR buffer [10×], 0.8 µL of MgCl₂ [50 mM], 0.4 µL of dNTP [10 mM] and 0.1 µL of BIOTAQ polymerase [5 U/µL] (Eurobio AbCys). The thermal profile consisted of an initial denaturation (94 °C, 3 min), followed by 35 cycles of denaturation (94 °C, 30 s), annealing (45 to 55 °C, 45 s) and extension (72 °C, 2 min), and a final extension (72 °C, 10 min) step. The PCR products were separated on a 1.5% agarose gel, purified with the GeneClean kit (MP Biomedicals), and cloned into a pBluescript KS plasmid vector using the T4 DNA ligase (Thermo Fisher Scientific). The ligation product was introduced in competent *Escherichia coli* cells (DH5alpha) that were cultured at 37 °C overnight. The clone screening was performed through PstI/HindIII (Thermo Fisher Scientific) digestion of plasmid DNA after plasmid extraction. Positive clones were sequenced on both strands (GATC Biotech). The resulting nucleotide sequences were deposited in the GenBank database under the accession numbers KU726988 (*M. fortunata* IR25a; consensus sequence from 6 clones), KU726987 (*R. exoculata* IR25a; consensus sequence from 3 clones), KU726989 (*C. chacei* IR25a; consensus sequence from 4 clones), KU726990 (*A. markensis* IR25a; consensus sequence from 4 clones), KU726984 (*P. elegans* IR25a; consensus sequence from 11 clones), KU726985 (*P. varians* IR25a; consensus sequence from 12 clones), and KU726986 (*P. serratus* IR25a; consensus sequence from 3 clones). Specific primers were further designed to amplify IR25a sequences in diverse tissues of the 4 alvinocaridid species and the palaemonid *P. elegans* (Supplementary Table S1). PCR amplifications were performed using BIOTAQ polymerase (Eurobio, AbCys) in a thermocycler (Eppendorf, Hamburg, Germany) with the following program: 94 °C for 3 min, 35 cycles of (94 °C for 30 s, 55 °C for 45 s, 72 °C for 2 min), and 72 °C for 10 min, with minor modifications of annealing temperature for different primer pairs.

Sequence analyses

A dataset of IR amino acid sequences was created, including the IR25a sequences identified in shrimp (present study), in other decapods (*P. argus*, Corey et al. 2013; *C. clypeatus*, Groh-Lunow et al. 2015; *H. americanus* AY098942, Hollins et al. 2003) and

Table 1. Cruises, locations and depths of the different sampling sites of the samples used in this study

Sites	Lat.	Long.	Depth (m)	Cruise, year	Ship/ submersible	Chief scientist
Menez Gwen	37°51'N	31°31'W	840	Biobaz, 2013	Pourquoi Pas? / ROV Victor	F. Lallier
Lucky Strike	37°17'N	32°16'W	1700	Biobaz, 2013	Pourquoi Pas? / ROV Victor	F. Lallier
				Momarsat, 2011	Pourquoi Pas? / ROV Victor	M. Cannat
				Momarsat, 2012	Thalassa / ROV Victor	M. Cannat and P. M. Sarradin
Rainbow	36°13'N	33°54'W	2260	Biobaz, 2013	Pourquoi Pas? / ROV Victor	F. Lallier
TAG	26°08'N	44°49'W	3600	Bicose, 2014	Pourquoi Pas? / ROV Victor	M. A. Cambon-Bonavita
Snake Pit	23°23'N	44°58'W	3480	Bicose, 2014	Pourquoi Pas? / ROV Victor	M. A. Cambon-Bonavita

in other crustaceans (*D. pulex*, Croset et al. 2010; *L. salmonis* PRJNA280127) together with IR sequences from the insects *B. mori*, *D. melanogaster*, *A. mellifera*, and *T. castaneum* (Croset et al. 2010). *Drosophila melanogaster* ionotropic glutamate receptor sequences were also included to serve as an out-group, and the final data set contained 173 sequences. These amino acid sequences were aligned with MAFFT v.6 (Katoh and Toh 2010) using the FFT-NS-2 algorithm and default parameters. The alignment was then manually curated to remove highly divergent regions (500 amino acid positions conserved in the final dataset). The phylogenetic reconstruction was carried out using maximum-likelihood. The LG+I+G+F substitution model (Le and Gascuel 2008) was determined as the best-fit model of protein evolution by ProtTest 1.3 (Abascal et al. 2005) following Akaike information criterion. Rate heterogeneity was set at 4 categories, and the gamma distribution parameter was estimated from the data set. Tree reconstruction was performed using PhyML 3.0 (Guindon et al. 2010), with both Subtree Pruning and Regrafting (SPR) and Nearest Neighbour Interchange (NNI) methods for tree topology improvement. Branch support was estimated by approximate likelihood-ratio test (aLRT) (Anisimova et al. 2006). Images were created using the iTOL web server (Letunic and Bork 2011).

Results

Morphology of the chemosensory organs: description and distribution of setal types on the antennae and antennules

In the 5 shrimp species studied for morphology (*P. elegans*, *M. fortunata*, *R. exoculata*, *C. chacei*, and *A. markensis*), antennae and antennules both consist of a peduncle and segmented flagella (one for the antennae and 2 for the antennules: an outer or lateral, and an inner or medial). In the 3 flagella, the diameter and length of the annuli vary, being large and short at the base and becoming thinner and longer towards the apex. The aesthetasc dimensions vary also along the flagella, being thinner and shorter at the base and growing toward the apex. The set of values (maximum, minimum, mean and standard deviation of diameter and length) for aesthetasc, as well as for non-aesthetasc sensilla, are given in Supplementary Table S2.

Palaemon elegans

The antennules are made of 3 basal annuli and 2 distal flagella. The lateral flagella are divided in 2 rami after a short fused basal part: a long external one and a shorter internal one (1/3 of the long one, $n = 12$, SD = 0.61) (Figure 1A). The aesthetascs are localized

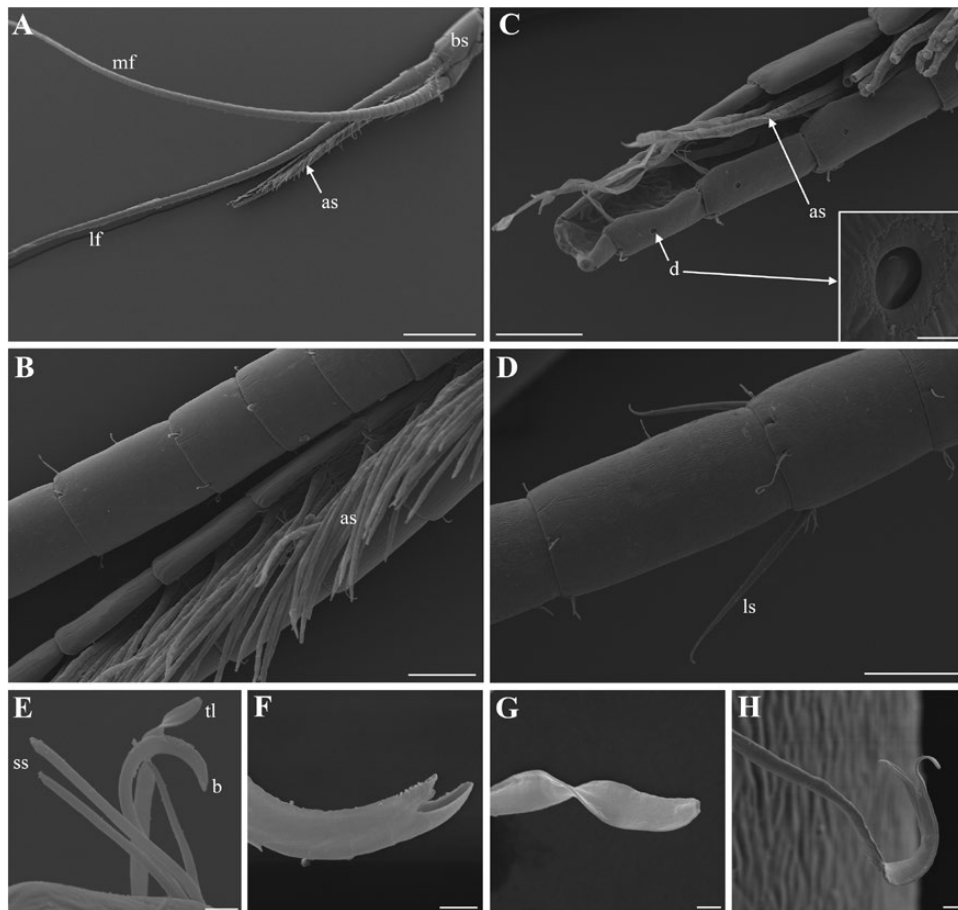


Figure 1. Morphology of antennules and setal types of *Palaemon elegans*. (A) Antennules are made of 3 basal annuli (bs) and 2 flagella: a medial (mf) and a lateral one (lf), which is divided in 2 rami: a long (outer) and a short (inner), bearing the aesthetascs (as). (B) Close-up on the ventral side of the furrow on the shorter ramus of the lateral flagellum bearing the aesthetascs. (C) Apex of the shorter ramus, showing the absence of aesthetascs on the last 2 annuli and the occurrence of small cuticular depressions (d), enlarged in insert. (D) Medial antennular flagellum showing the long simple seta (ls). (E) Tuft of 3 simple short (ss), one twisted flat (tf) and one beaked scaly (b) setae. (F) Beaked scaly seta. (G) Twisted flat seta. (H) Bifid seta. Scale bars: A = 1 mm; B, C, D = 100 μ m; E = 10 μ m; F, G, H = 2 μ m. Scale bar in insert in C = 5 μ m.

ventrally, in a furrow on the shorter ramus (Figure 1B). They are present from the basal fused part of the antennules to the apex of the short ramus (except from the last 2 annuli, Figure 1C). Two rows of 5 to 6 aesthetascs occur on each annulus (one row at the distal part of the annulus and the other at the middle part) (Figure 1B). The 2 or 3 basal and apical annuli have a smaller number of aesthetascs, giving a total number of approximately 140 aesthetascs per ramus (Table 2). Aesthetascs are up to 20.3 μm in diameter ($n = 14$) and 393 μm in length ($n = 10$) (Supplementary Table S2). They bear annulation throughout their length (short at the base and longer towards the apex), and lack a terminal pore.

Non-aesthetasc setae are also present on all the annuli of the 3 flagella (antennae and antennules), where they are distributed (up to 8) around the distal part of each annulus (Figure 1D). Five setal types are observed on the flagella, named after their morphology (dimensions are given in Table 2): 1) short simple seta (Figure 1E), 2) long simple seta (Figure 1D), 3) beaked scaly seta (Figure 1F), 4) twisted flat seta (Figure 1G), and 5) bifid seta (Figure 1H). All these 5 types appear to have a terminal pore. Short simple, beaked scaly and twisted flat setae are present on the antennae, the medial flagella of the antennules and the long ramus of the lateral flagella of the antennules. They occur as tufts of 5 setae, containing 3 simple short, one twisted flat and one beaked scaly seta (Figure 1E). These tufts are present on each annulus near the base but are spaced further apart towards the apex. The bifid setae are found only on the 2 flagella of the antennules, whereas the long simple are only found on medial flagella of the antennules (2 every 5 annuli, on each side of the flagellum). Small round cuticular depressions (5.5 to 6.7 μm in diameter) are observed on the medial side of the short ramus of the lateral flagella of the antennules, as well as on the antennae (insert in Figure 1C).

Mirocaris fortunata

In *M. fortunata*, as well as in the 3 other hydrothermal species, the antennules are also made of 3 basal annuli and 2 distal flagella (lateral and medial) (Figure 2A). In *M. fortunata*, the aesthetascs are

localized latero-ventrally on the inner side of the lateral flagella, from the base to 2/3 of the flagella. One row of 3 to 4 aesthetascs occurs on the distal part of each annulus (Figure 2B), leading to a total number of approximately 60 aesthetascs per ramus (Table 2). Aesthetascs are up to 18.3 μm in diameter ($n = 21$) and 290.3 μm in length ($n = 46$) (Supplementary Table S2). They bear annulation on the apical half, and lack a terminal pore.

The rows of aesthetascs are flanked on the inner side by non-aesthetasc setae, organized as follows: one intermediate seta (thinner and shorter than the aesthetascs) and 2 or 3 short thin setae (thinner and shorter than the former) (Figure 2B). The intermediate setae have a peculiar apex shape with no obviously visible pore (Figure 2D), whereas the short setae are simple with a clearly visible pore at the apex (Figure 2E).

Intermediate and short simple setae also occur along with a sparse third type of non-aesthetasc setae (Figure 2F) on the 2 other flagella (medial flagella of the antennules and the antennae), distributed around the distal part of each annulus (about 10 over the entire circumference by extrapolation of what is seen on one face). Small round cuticular depressions (7 to 10 μm in diameter) are observed on the lateral flagella of the antennules, on the medial side of the aesthetascs (Figure 2B). Flagella are often densely covered by a thick bacterial layer of filamentous and rod-shaped bacteria (Figure 2C), which was never observed on *P. elegans*. Rod-shaped bacteria also sometimes covered the entire aesthetasc surface (not shown).

Rimicaris exoculata

The aesthetascs are localized laterally on the medial side of the lateral flagella, from the base (except the 2 or 3 first annuli) up to the apex (except for the 4 last annuli). One row of 3 to 4 aesthetascs occurs on the distal part of each annulus (Figure 3A), leading to a total number of approximately 108 aesthetascs per ramus. Aesthetascs are up to 22 μm in diameter ($n = 22$) and 191 μm in length ($n = 26$) (Supplementary Table S2). They bear annulation on the apical half, and lack a terminal pore.

Table 2. Comparative table of aesthetascs setae characteristics in different species of decapods

Species	Total number	Number per row	Dimensions (diameter \times length in μm)	Reference
Lobster				
<i>Panulirus argus</i> (20–60 cm)	2000 to 4000	9–10	40 \times 1000	Gleeson et al. 1993 Laverack 1964
<i>Homarus americanus</i> (20–60 cm)	2000	10–12	20 \times 600	Guenther and Atema 1998
Crayfish				
<i>Orconectes propinquus</i> (4–10 cm)	160	3–6	12 \times 150	Tierney et al. 1986
<i>Cherax destructor</i> (10–20 cm)	260 ^a	2–5	18 \times 100	Sandeman and Sandeman 1996 Beltz et al. 2003
Crab				
<i>Callinectes sapidus</i> (23 cm)	1400	~20	12 \times 795	Gleeson et al. 1996
<i>Carcinus maenas</i> (9 cm)	100–300	8–10	13 \times 750	Fontaine et al. 1982
Shrimp				
<i>Lysmata</i> ^b (5–7 cm)	210–460	3–5	20 \times 800	Zhang et al. 2008
<i>Palaemon elegans</i> (7 cm)	280	5–6	14 \times 230	This study
<i>Mirocaris fortunata</i> (3 cm)	120 ^a	3–4	16 \times 234	This study
<i>Rimicaris exoculata</i> (5.5 cm)	206 ^a	3–4	20 \times 170	This study
<i>Chorocaris chacei</i> (5.5 cm)	226 ^a	2–4	19 \times 251	This study
<i>Alvimocaris markensis</i> (8.2 cm)	220 ^a	3–4	21 \times 531	This study

Rough animal lengths are given for comparison. Total length is given for lobster, crayfish and shrimp, carapace width for crabs.

^aSpecies with only one row of aesthetascs per annuli.

^bStudy realized on *Lysmata boggei*, *L. wurdemanni*, *L. amboinensis*, and *L. debelii*.

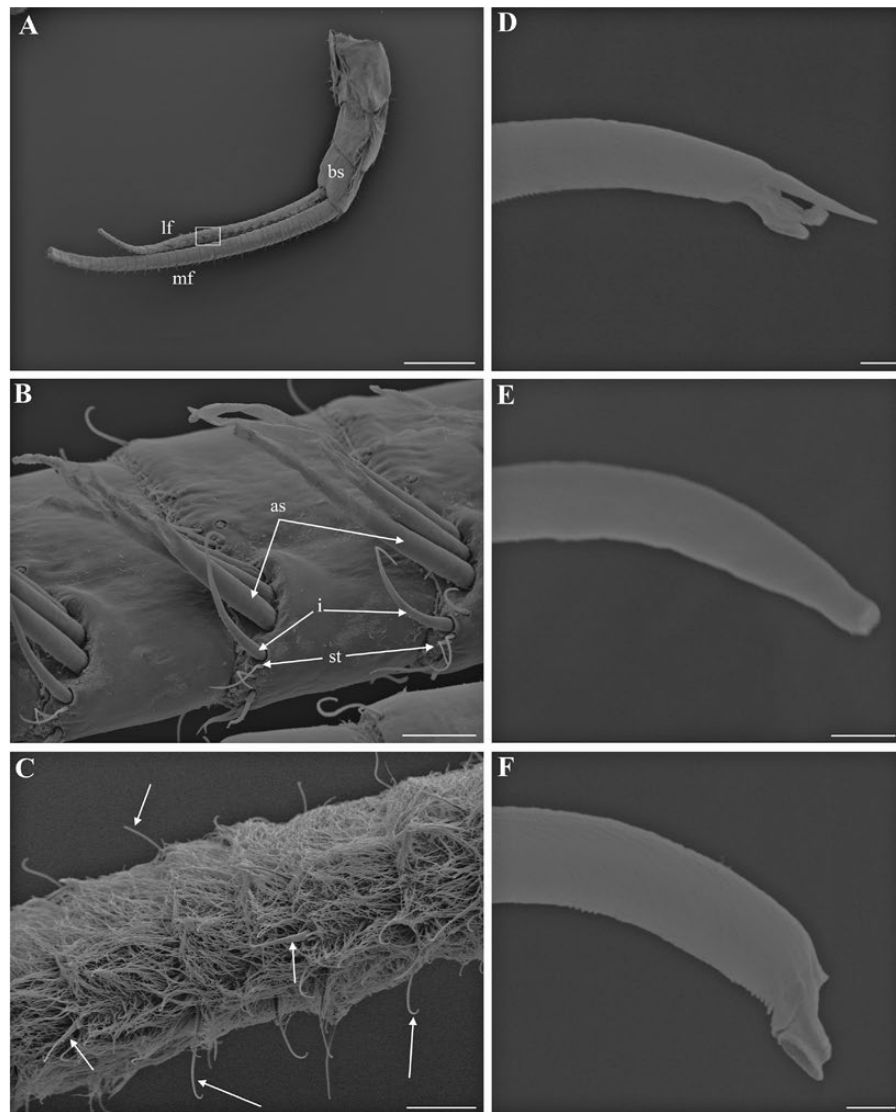


Figure 2. Morphology of antennule and setal types of *Mirocaris fortunata*. (A) Antennules are made of 3 basal annuli (bs) and 2 flagella: a medial (mf) and a lateral one (lf), bearing the aesthetascs (as). Box: area enlarged in B. (B) Close-up on the lateral flagellum bearing the aesthetascs, and intermediate (i) and short thin setae (st). (C) Lateral flagellum covered by dense filamentous and rod-shaped bacteria. Some setae are visible, protruding from the layer of bacteria (arrows). (D) Apex of the intermediate simple setae. (E) Short setae are simple with a clear pore at the apex. (F) Third setal type. Scale bars: A = 1 mm; B = 50 μ m; C = 100 μ m; D, E, F = 1 μ m

The arrangement pattern of the non-aesthetasc setae around the aesthetascs is quite similar to that observed in *M. fortunata*, but with different setal types: 1 long thick beaked seta, 1 intermediate beaked seta and 6 or 7 short thin beaked setae (Figure 3B). All these setae have a pore at the apex (Figure 3C), but they are devoid of scales unlike the beaked setae observed in *P. elegans*.

Long thick, intermediate and short thin beaked setae also occur on the outer side of the lateral flagella, on the medial flagella of the antennules, and on the antennae, distributed over the circumference (20–25 over the entire circumference by extrapolation of setae seen on one face, or counted on the periphery of the apex), with a tight tuft of 6–8 setae on the inner side.

Small round cuticular depressions were (rarely) observed (6 to 8 μ m in diameter) in *R. exoculata*, but they are barely observable due to a dense rod-shaped bacterial coverage. Indeed, for this species too, we have observed that the flagella (even the aesthetascs) can be covered by layer of filamentous and rod-shaped bacteria (not shown).

Chorocaris chacei

The aesthetascs are localized laterally on the medial side of the lateral flagella, from the base (except the 4 or 5 first annuli) to 2/3 of the flagella. One row of 2 to 4 aesthetascs occurs on the distal part of each annulus (Figure 3D), leading to a total number of approximately 113 aesthetascs per ramus. Aesthetascs are up to 23.2 μ m in diameter ($n = 50$) and 339.5 μ m in length ($n = 58$) (Supplementary Table S2). They bear annulation on the apical half, and lack a terminal pore.

The arrangement pattern of the non-aesthetasc setae around the aesthetascs is also quite similar to that observed in *M. fortunata* with one intermediate beaked seta, and 1 to 3 short simple or beaked setae on both the medial and lateral sides (Figures 3E and F).

Intermediate beaked and short setae (either simple or beaked shaped) also occur on the medial flagella of the antennules, and on the antennae, distributed over the circumference, roughly equidistant (around 15 over the entire circumference by extrapolation of

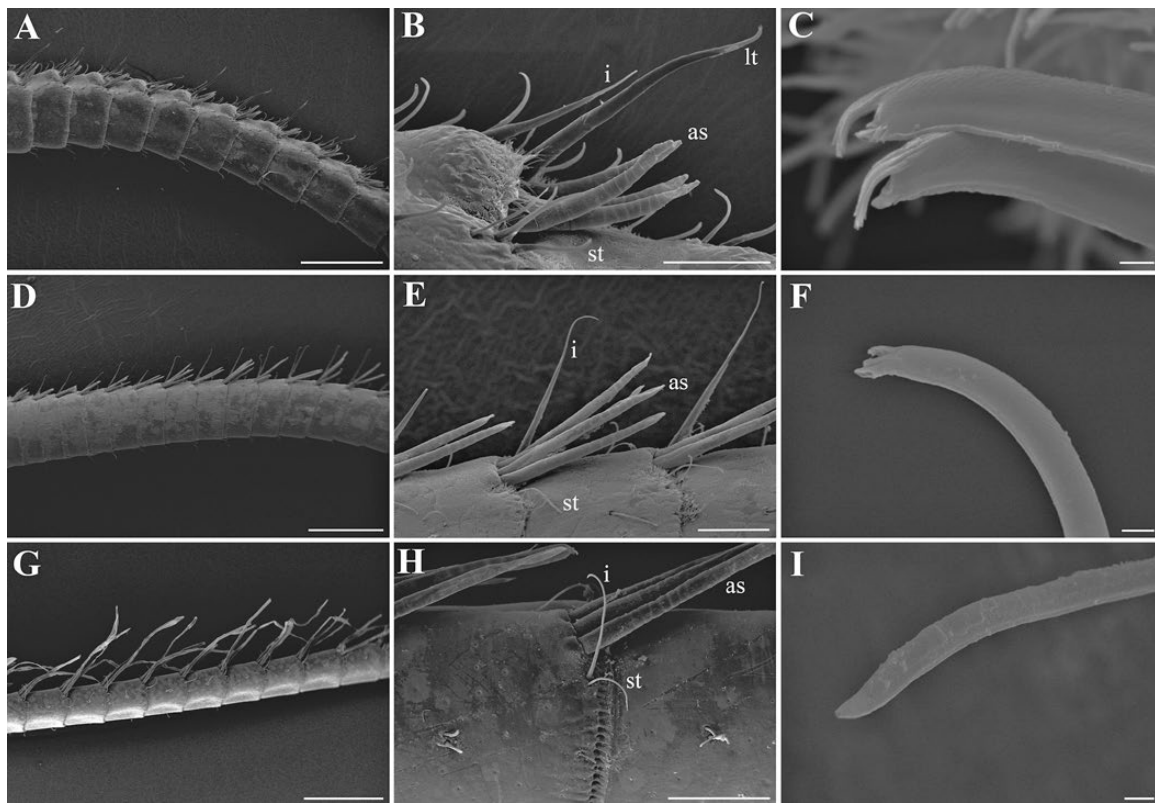


Figure 3. Morphology of lateral flagella and setal types of *Rimicaris exoculata* (A, B, C), *Chorocaris chacei* (D, E, F) and *Alvinocaris markensis* (G, H, I). as: aesthetascs, lt: long thick seta, i: intermediate seta, st: short thin seta, Scale bars: A, D, G = 500 μm ; B, E, H = 100 μm ; C, F, I = 2 μm .

setae seen on one face, or counted on the periphery of the apex), with a tight tuft of 8 to 10 setae on the inner side.

Small cuticular depressions (5 to 5.5 μm in diameter) are observed on the lateral flagella of the antennules, on the medial side of the aesthetascs but are difficult to observe as they are covered by rod-shaped bacteria. For this species again, the flagella (and even the aesthetascs) can be covered by filamentous and rod-shaped bacteria (not shown).

Alvinocaris markensis

The aesthetascs are localized laterally on the medial side of the lateral flagella, from the base (except the 3 or 4 first annuli) up to half of the flagella. One row of 3 to 4 aesthetascs (rarely 5) occurs on the distal part of each annulus (Figure 3G), leading to a total number of approximately 110 aesthetascs per ramus. Aesthetascs are up to 25.2 μm in diameter ($n = 39$) and 879.1 μm in length ($n = 49$) (Supplementary Table S2). They bear annulation almost throughout their length (short at the base and longer towards the apex), and lack a terminal pore.

The arrangement pattern of the non-aesthetasc setae around the aesthetascs is quite similar to that observed in *M. fortunata* with 1 intermediate seta and 1 short thin seta (Figure 3H). Two (sometimes 3 or 4) short setae occur at mid-length of each annulus. Intermediate and short thin setae all seem to all be simple, with a pore (Figure 3I). They also occur on the medial flagella of the antennules and on the antennae, in fewer numbers than observed in the other species (4–6 over the entire circumference, mostly on the medial side). Long simple setae also occur on few basal annuli on the medial flagella of the antennules and of the antennae.

Small cuticular depressions (4.5 to 7.5 μm diameter) were also observed in *A. markensis*, on the lateral flagella of the antennules,

on the distal part of the annuli, occurring by one, 2 or sometimes 3, which had not been observed in other species (not shown). They are also observed on the antennae. Only a few rod-shaped bacteria occurred on the 2 specimens observed.

Identification and expression of the putative olfactory co-receptor IR25a in hydrothermal vent and coastal shrimp

In order to identify the regions of antennules and antennae putatively involved in olfaction, we studied the expression pattern of the IR 25a, which belongs to a conserved family of olfactory receptors amongst Protostomia (review in Croset et al. 2010), involved in olfaction, taste, thermosensation, and hygrosensation. Recently the homologue of IR25a was identified in the lobster, and had been associated with olfactory sensilla (Corey et al. 2013). Using homology-based PCR with primers designed from the alignment of IR25a sequences from diverse organisms, we obtained partial sequences for 7 species of shrimp: 903 bp for *R. exoculata*, *P. elegans*, and *P. varians*, 763 bp for *M. fortunata*, *C. chacei*, and *A. markensis*, and 881 bp for *P. serratus* (Figures 4A and B). A phylogenetic analysis confirmed that these sequences are IR25a orthologs (Figure 5). All shrimp sequences grouped with IR25a sequences from other arthropods, and were closely related to IR25a sequences from the decapod crustaceans *P. argus* (Corey et al. 2013), *H. americanus* (Hollins et al. 2003) and *C. clypeatus* (Groh-Lunow et al. 2015). The Palaemonidae and Alvinocarididae sequences formed distinct clusters within the shrimp sequences, therefore being congruent with the phylogeny of these groups (Figure 6). The IR25a partial amino acid sequences obtained in this study are about 250 to 300 amino acids in length, which represents 25 to 30% of the total length expected for such sequences (Figure 4). They include the ligand-gated ion channel

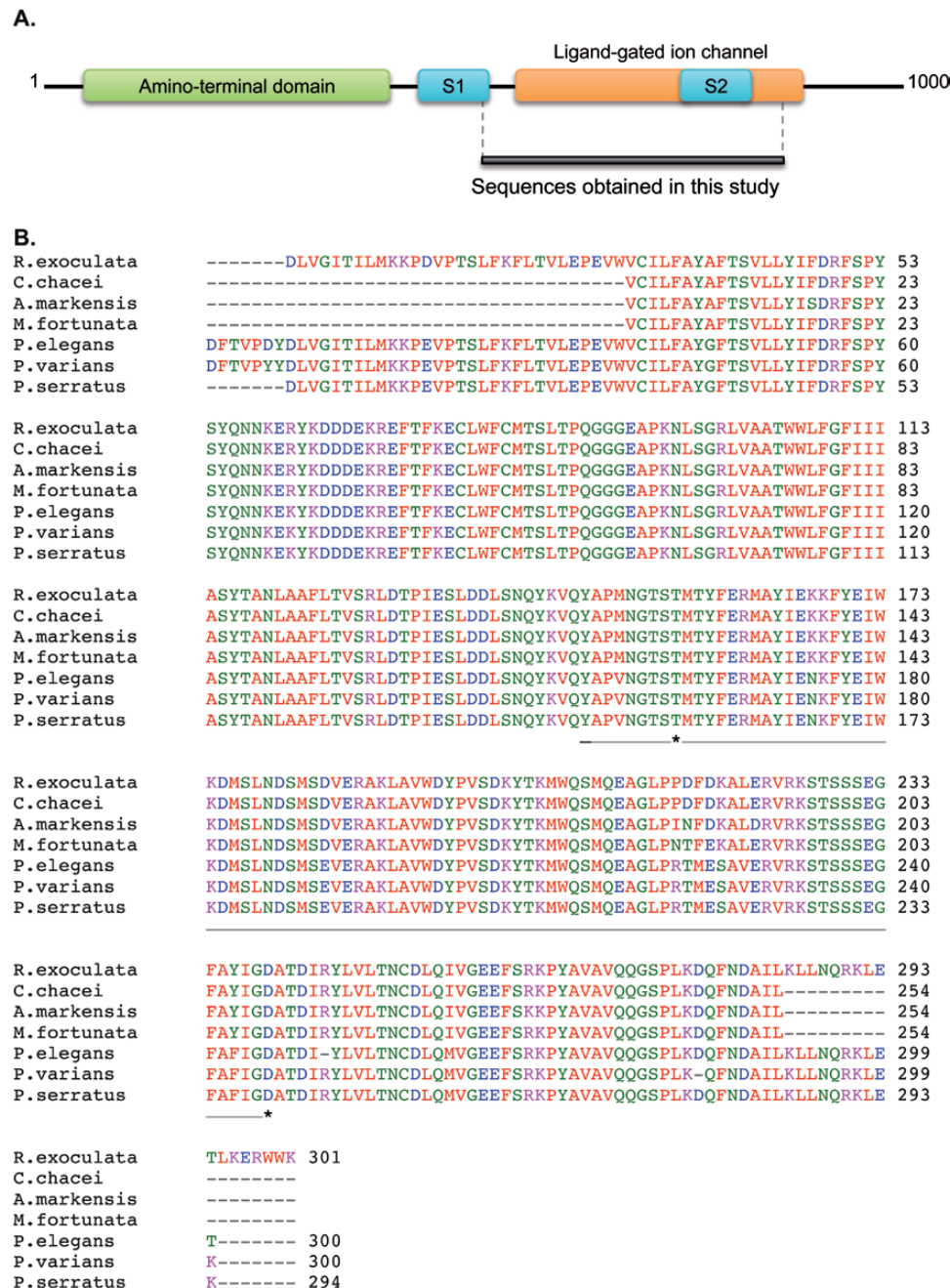


Figure 4. IR25a partial sequences obtained for hydrothermal and coastal shrimp. (A) IR25a protein domain organization (modified from Croset et al. 2010) showing the position of the shrimp partial sequences obtained in the present study. The ligand-binding domains are named S1 and S2. (B) Alignment of shrimp IR25a sequences. The ligand-binding S2 domain is underlined, and putative ligand-binding residues are indicated by an asterisk.

and the ligand-binding S2 domain, localized in the C-terminal part of the protein. When considering the ligand-binding S2 domain, the threonine and aspartate, which are characteristic glutamate binding residues, are conserved among shrimp sequences.

Then, we studied the expression pattern of IR25a in antennules, antennae, mouthparts and walking legs, as well as in non-chemosensory tissues (abdominal muscles, eye), from the 4 hydrothermal vent shrimp and the coastal shrimp *P. elegans* (Figure 7). IR25a was predominantly expressed in the lateral antennular flagella (A1 lateral) for all shrimp. In *P. elegans*, a weaker expression was observed in the external ramus (A1 lateral R2) than in the internal ramus of the lateral antennular flagella (A1 lateral R1), which bear the aesthetascs.

A weak expression was also detected in the medial antennular flagella of *R. exoculata* and *C. chacei* (A1 medial), and in the antennae (A2) of *R. exoculata*. IR25a transcripts were undetectable in other tissues.

Discussion

Comparative morphology of sensilla of antennae and antennules among decapods, and in coastal palaemonid versus hydrothermal alvinocarid shrimp. Setae are outgrowths of the arthropod integument presenting a multitude of sizes and shapes. These ubiquitous features of crustacean

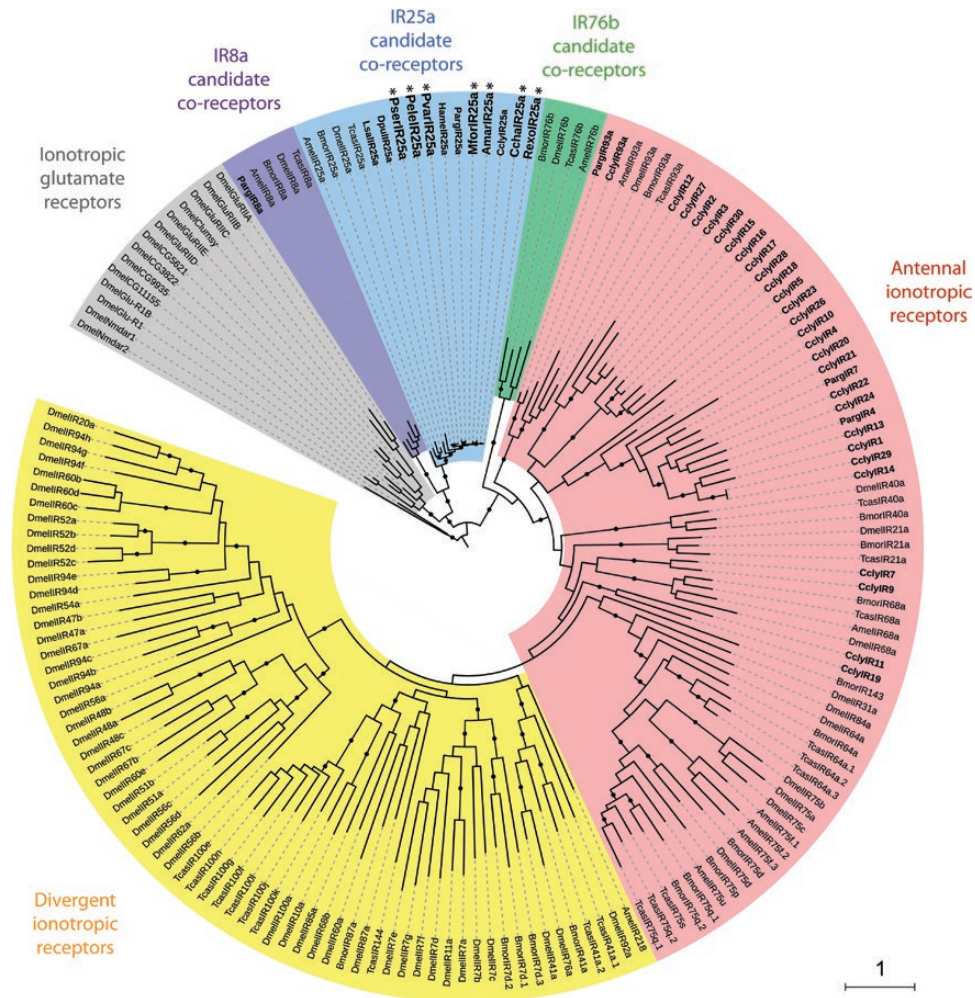


Figure 5. Phylogeny of insect and crustacean ionotropic receptors (IRs). This tree is based on a maximum-likelihood analysis of an amino acid dataset. *Drosophila melanogaster* ionotropic glutamate receptor sequences were used as an out-group. Branch support was estimated by approximate likelihood-ratio test (aLRT) (circles: >0.9). The scale bar corresponds to the expected number of amino acid substitutions per site. Crustacean IRs are in bold and the new IRs identified in this study are in larger font size, and highlighted with an asterisk. Amar, *Alvinocaris markensis*; Amel, *Apis mellifera*; Bmor, *Bombyx mori*; Ccha, *Chorocaris chacei*; Ccly, *Coenobitus clypeatus*; Dmel, *Drosophila melanogaster*; Dpul, *Daphnia pulex*; Hame, *Homarus americanus*; Lsal, *Lepeophtheirus salmonis*; Mfor, *Mirocaris fortunata*; Parg, *Panulirus argus*; Pele, *Palaemon elegans*; Pser, *Palaemon serratus*; Pvari, *Palaemon varians*; Rexo, *Rimicaris exoculata*; Tcas, *Tribolium castaneum*.

integuments are involved in a variety of vital functions including locomotion, feeding, sensory perception and grooming (Felgenhauer 1992). Sensilla (setae innervated by sensory cells) were shown to present a great inter- and intra-specific diversity in crustaceans (see references in the paragraphs below).

In the most studied large decapods like lobsters and crayfish, the aesthetascs are localized in tufts on the distal half or two-thirds of the ventral side of each lateral antennular flagellum (*P. argus*, Cate and Derby 2001; *H. americanus*, Guenther and Atema 1998; *Orconectes sanborni*, McCall and Mead 2008; *O. propinquus*, Tierney et al. 1986; *Procambarus clarkii*, Mellon 2012). The localization at the tip of the antennules may increase the spatial resolution of the chemical environment, but could also increase their chance of damage during encounters with the environment or other animals. On the contrary, in shrimp (the 4 alvinocaridid species and *P. elegans* [this study], as well as other palaemonid species like *P. serratus* and *Macrobrachium rosenbergii* [Hallberg et al. 1992]), the aesthetascs are localized on the basal half or two-thirds of the lateral flagella (for the alvinocarididae) or on the basal part of the short ramus of the lateral flagella

(for the palaemonidae). The aesthetascs are thus less likely to be lost or damaged, but this arrangement may decrease spatial resolution.

The aesthetascs are usually organized in 2 successive rows (in the different lobsters and crayfishes cited above and also in *Lysmata* shrimp, Zhang et al. 2008) or in 2 juxtaposed rows in the short antennules of the crab *Carcinus maenas* (Fontaine et al. 1982). Surprisingly, there is only one row of aesthetascs on each annulus in the 4 hydrothermal species (an exception also occurs in the crayfish *Cherax destructor*, see Table 2). Nevertheless, comparisons of the total number of aesthetascs in diverse decapod species (Table 2) revealed that this number is relatively similar among shrimp group and other decapods of comparable size (the crayfish *Orconectes propinquus* or the crab *C. maenas*) (Table 2 and see Beltz et al. 2003 for more comprehensive data). Hydrothermal shrimp do not seem to present any specific adaptation regarding this character. The total number, as well as the size of aesthetascs seems related to the size of the animal rather than to its environment. Indeed, based on a study of 17 Reptentia decapods, Beltz et al. (2003) found a strong linear relationship between the number of aesthetascs and carapace

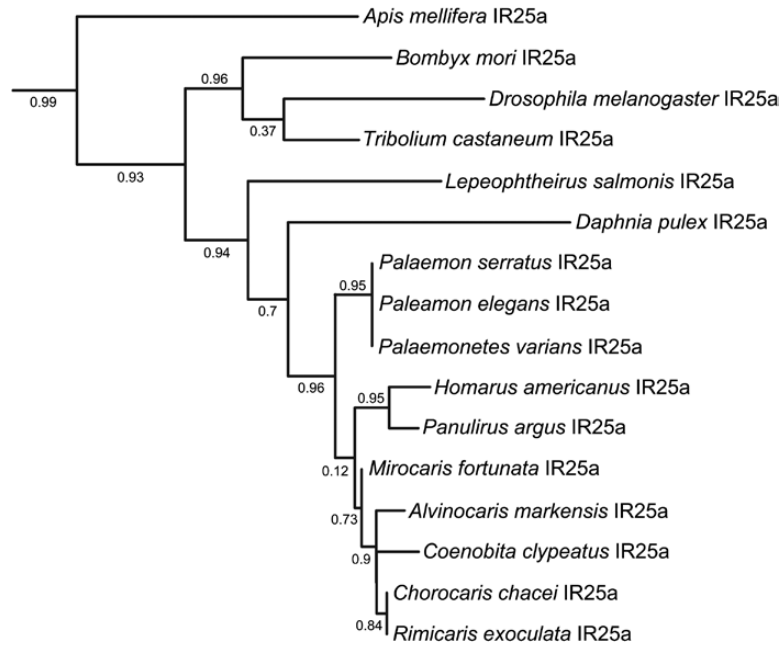


Figure 6. Detail of the IR25a clade of the IR phylogeny. This sub-tree is a zoom of the IR25a clade from the tree depicted in Figure 5.

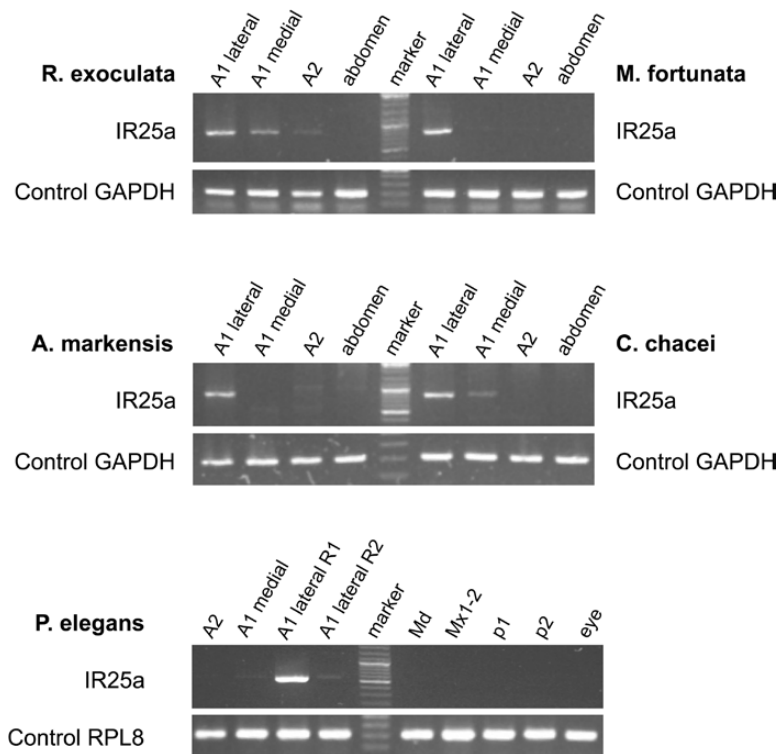


Figure 7. IR25a gene expression in hydrothermal vent shrimp *Rimicaris exoculata*, *Mirocaris fortunata*, *Alvinocaris markensis*, *Chorocaris chacei*, and in the coastal shrimp *P. elegans*. Control RT-PCR products for comparative analysis of gene expression correspond to the glycolysis enzyme GAPDH for hydrothermal vent shrimp, and to the ribosomal protein gene RPL8 for *P. elegans*. No amplification was detected in the absence of template (data not shown). A1, antennules; R1, internal ramus of the lateral antennular flagella; R2, external ramus of the lateral antennular flagella; A2, second antennae; Md, mandibles; Mx1-2, maxillae; p1 and p2, first and second walking legs.

length, which was also reported earlier for the crayfish *C. destructor* by Sandeman and Sandeman (1996). Among hydrothermal species, it can however be noted that the aesthetascs of *A. markensis* are longer than those of the 3 other species, with the maximum length being

2 to 4 times higher than for the 3 other species (see Supplementary Table S2). The adult hydrothermal shrimp lack the usual externally differentiated eye (eye-stalked), having instead a pair of large, highly reflective, dorsal organs (Van Dover et al. 1989). These modifications

have been reported to be an adaptation for the detection of extremely faint sources of light emitted by the vents (Pelli and Chamberlain 1989). These eyes are unusual in having no image-forming optics, but a solid wall of light-sensitive rhabdom containing rhodopsin, with the exception of *A. markensis*, which also lacks this photoreceptor and is completely blind (Wharton et al. 1997; Gaten et al. 1998). The longer olfactory sensilla observed in this species may possibly be interpreted as a development of the olfactory capacity to compensate for the lack of vision. Zhang et al. (2008) showed for *Lysmata* species that shrimp living in aggregations (*L. boggei* and *L. wurdemanni*, 460 aesthetascs) possess a significantly higher number of aesthetascs than pair-living species (*L. amboinensis* and *L. debelius*, 210 aesthetascs), suggesting a possible correlation between the number of aesthetascs and the social behavior. Our results do not support this hypothesis, since no significant differences were observed between vent species living in dense swarms (*R. exoculata*) and the others.

Most studies on olfaction in crustaceans have focused on aesthetascs. Several lines of evidence however suggest that non-aesthetasc bimodal chemosensilla (innervated by mechano- and chemo-receptive cells, also called distributed chemosensilla [Schmidt and Mellon 2011]) or non-olfactory sensilla (Derby and Weissburg 2014), distributed over both flagella of the antennules, as well as on the antennae, also play a role in the detection of water-borne chemicals (Guenther and Atema 1998; Cate and Derby 2001). Non-aesthetasc setae exhibit a wide variety of sizes and morphologies. These setae are named in the literature according to their morphology, size or location on the flagellum. For example, there are 9 setal types in *P. argus* (hooded, plumose, short setuled, long simple, medium simple, short simple, guard, companion, and asymmetric; Cate and Derby 2001), but only 1 type in the shrimp *Thor manningi* (curved simple; Bauer and Caskey 2006). The role of these setae is still poorly known and whether their diversity corresponds to a multiplicity of perceived stimuli remains an open question (Cate and Derby 2001; Derby and Steullet 2001). Among the shrimp studied here, the coastal shrimp *P. elegans* showed the highest diversity in non-aesthetasc setal types (5 setal types: short simple, long simple, beaked scaly, twisted flat, bifid) when compared with the 4 hydrothermal species (2 or 3 types). Among hydrothermal species, the setal types vary essentially by their size (long, intermediate or short) and less by their morphology (all simple in *Alvinocaris*, all beaked in *Rimicaris*, a mix of the 2 in *Chorocaris*, whereas *Mirocaris* exhibit more original morphologies [see Figures 2D and 2F]). At this point of our knowledge, it is difficult to explain the observed differences and even more to speculate on the functions of these different setae.

Surprisingly, dense bacterial populations were often observed on the antennae and antennules of the 4 hydrothermal shrimp (see e.g., *Mirocaris*, Figure 2C), sometimes even covering the whole surface of aesthetascs (not shown), whereas no bacterial coverage was ever observed in the coastal *P. elegans* specimens. The type of bacteria present on the antennae of hydrothermal shrimp, as well as their potential impact on olfaction or other role for the shrimp should be investigated in future studies.

Comparative expression of the putative olfactory co-receptor IR25a in hydrothermal vent and coastal shrimp

We identified, in the 4 alvinocaridid hydrothermal shrimp and in 3 palaemonid species (*P. elegans*, *P. varians*, and *P. serratus*), a member of the IR family, which was recently proposed to be involved in the odorant detection in crustaceans: the common IR25a subunit

(Corey et al. 2013). In the 5 shrimp species tested, IR25a was predominantly expressed in the lateral antennular flagella that bear the aesthetascs olfactory sensilla (Figure 7), consistent with the expression pattern of this IR subunit in *H. americanus* (iGluR1, Stepanyan et al. 2004), *P. argus* (Corey et al. 2013), and *C. clypeatus* (Groh-Lunow et al. 2015). IR25a expression in other chemosensory tissues than the lateral antennular flagella varies amongst decapod crustacean species, with either no detection (for *M. fortunata*, *A. markensis*, *P. elegans*: this study; for *H. americanus*: Stepanyan et al. 2004), or detection in different organs (medial antennular flagella in *R. exoculata* and *C. chacei*: this study; mouth and 2 first walking legs in *P. argus*: Corey et al. 2013). Taken together, these results raise the question of whether IR25a may play a more general role in decapod crustacean chemosensation beyond just mediating odor detection (Corey et al. 2013), or if organs other than the aesthetascs bearing flagella can also have an olfactory role, as Keller et al. (2003) suggested for the antennae and walking legs of the blue crab *Callinectes sapidus*. According to several recent studies and reviews (Schmidt and Mellon 2011, Mellon 2014; Derby and Weissburg 2014; Derby et al. 2016), only the aesthetascs are considered as olfactory sensilla, which rather plead for the first hypothesis.

Among hydrothermal species, the different patterns of IR25a expression obtained for *R. exoculata* and *C. chacei* on one hand and for *M. fortunata* and *A. markensis* on the other hand, would suggest different chemosensory mechanisms in these 2 shrimp groups. This may be related to their diet and thus to their direct dependence to the hydrothermal fluid. Indeed, *Rimicaris* and *Chorocaris* to a lesser extent live in symbiosis with chemoautotrophic bacteria from which they derive all or part of their food (Segonzac et al. 1993; Ponsard et al. 2013), forcing them to stay permanently close to hydrothermal emissions to supply their bacteria in reduced compounds necessary for chemosynthesis. These 2 species are also phylogenetically closely related, which recently led Vereshchaka et al. (2015) to propose to synonymize all the genus *Chorocaris* with *Rimicaris*. On the other hand, *Mirocaris* and *Alvinocaris* are secondary consumers, scavenging on local organic matter and living at greater distances from the vent emissions. Regarding the IR25a expression pattern, the coastal shrimp *P. elegans* has a profile similar to hydrothermal secondary consumers *Mirocaris* and *Alvinocaris*, itself having an opportunistic omnivorous diet of invertebrate tissues.

In future studies, we will attempt to identify, and subsequently localize, other receptors of the IR family that could be involved in olfaction, and in particular the members generally found associated with IR25a (like IR93a and IR8a). We recently developed an electrophysiological method that allows the recording of shrimp ORNs activity (Machon et al. 2016). This method will be used to conduct a comparative study of the global antennule activity upon exposure to environmental stimuli, in the hydrothermal species *M. fortunata* and the coastal species *P. elegans*. An ultrastructural approach could help to refine the morphological comparison between hydrothermal and coastal species, by analyzing other characteristics like the number of ORNs per aesthetascs, the number of outer dendritic segments per ORNs or the aesthetasc cuticle thickness. This combined morphological and functional approach will provide insights into deep-sea vent shrimp olfaction, and ultimately in the potential adaptations of the sensory organs to their peculiar environment.

Supplementary Material

Supplementary data are available at *Chemical Senses* online.

Funding

This work was supported by the European Union Seventh Framework Programme (FP7/2007–2013) under the MIDAS project [grant agreement n° 603418].

Acknowledgments

The authors thank the electronic microscopy platform of the Institute of Biology Paris-Seine (IBPS), and especially V. Bazin and M. Trichet. We also thank the 2 chief scientist of the Momarsat 2011 and 2012 cruise M. Cannat and P. M. Sarradin, the chief scientist of the Biobaz 2013 (F. Lallier) and the Bicosé 2014 (MA Cambon-Bonavita) cruises, as well as Jozée Sarrazin for hydrothermal shrimp sampling.

References

- Abascal F, Zardoya R, Posada D. 2005. ProtTest: selection of best-fit models of protein evolution. *Bioinformatics*. 21(9):2104–2105.
- Ache B. 1982. Chemoreception and thermoreception. In: Bliss D, editor, *The Biology of Crustacea*. Vol 3. New York: Academic Press. p. 369–398.
- Anisimova M, Gascuel O. 2006. Approximate likelihood-ratio test for branches: a fast, accurate, and powerful alternative. *Syst Biol*. 55(4):539–552.
- Bauer R, Caskey J. 2006. Flagellar setae of the second antennae in decapod shrimps: sexual dimorphism and possible role in detection of contact sex pheromones. *Invertebr Reprod Dev*. 49(1–2):51–60.
- Beltz BS, Kordas K, Lee MM, Long JB, Benton JL, Sandeman DC. 2003. Ecological, evolutionary, and functional correlates of sensilla number and glomerular density in the olfactory system of decapod crustaceans. *J Comp Neurol*. 455(2):260–269.
- Benton R, Vannice KS, Gomez-Diaz C, Voshall LB. 2009. Variant ionotropic glutamate receptors as chemosensory receptors in *Drosophila*. *Cell*. 136(1):149–162.
- Cate HS, Derby CD. 2001. Morphology and distribution of setae on the antennules of the Caribbean spiny lobster *Panulirus argus* reveal new types of bimodal chemo-mechanosensilla. *Cell Tissue Res*. 304(3):439–454.
- Chamberlain S, Battelle B, Herzog E, Jinks R, Kass L, Renninger G. 1996. *Sensory neurobiology of hydrothermal vent shrimp from the Mid-Atlantic Ridge*. Abstract. FARA-IR Mid-Atlantic Ridge Symposium. Reykjavik, Iceland.
- Corey EA, Bobkov Y, Ukhanov K, Ache BW. 2013. Ionotropic crustacean olfactory receptors. *PLoS One*. 8(4):e60551.
- Cowan D. 1991. The role of olfaction in courtship behavior of the American lobster *Homarus americanus*. *Bio Bull*. 181:402–407.
- Croset V, Rytz R, Cummins SF, Budd A, Brawand D, Kaessmann H, Gibson TJ, Benton R. 2010. Ancient protostome origin of chemosensory ionotropic glutamate receptors and the evolution of insect taste and olfaction. *PLoS Genet*. 6(8):e1001064.
- De Busserolles F, Sarrazin J, Gauthier O, Gelinat Y, Fabri MC, Sarradin PM, Desbruyères D. 2009. Are spatial variations in the diets of hydrothermal fauna linked to local environmental conditions? *Deep-Sea Res II*. 56:1649–1664.
- Derby CD, Steullet P. 2001. Why do animals have so many receptors? The role of multiple chemosensors in animal perception. *Biol Bull*. 200(2):211–215.
- Derby C, Steullet P, Horner A, Cate H. 2001. The sensory basis of feeding behavior in the Caribbean spiny lobster, *Panulirus argus*. *Mar Freshwater Res*. 52:1339–1350.
- Derby C, Weissburg M. 2014. The chemical senses and chemosensory ecology of Crustaceans. In: Derby C, Thiel M, editors, *The Natural History of the Crustacea*. Vol. 3: *Nervous Systems and Control Behavior*. New York: Oxford Univ. Press. p. 263–292.
- Derby CD, Kozma MT, Senatore A, Schmidt M. 2016. Molecular mechanisms of perception and perireception in crustacean chemoreception: a comparative review. *Chem Senses*. 41(5):381–398.
- Desbruyères D, Almeida A, Biscoito M, Comtet T, Khripounoff A, Le Bris N, Sarradin PM, Segonzac M. 2000. A review of the distribution of hydrothermal vent communities along the northern Mid-Atlantic Ridge: dispersal vs. environmental controls. *Hydrobiologia*. 440:201–216.
- Desbruyères D, Biscoito M, Caprais JC, Colaço A, Comtet T, Crassous P, Fouquet Y, Khripounoff A, Le Bris N, Olu K, et al. 2001. Variations in deep-sea hydrothermal vent communities on the Mid-Atlantic Ridge near the Azores plateau. *Deep-Sea Res I*. 48:1325–1346.
- Desbruyères D, Segonzac M, Bright M. 2006. Handbook of deep-sea hydrothermal vent fauna. Second completely revised edition. Linz (Austria): Denisia.
- Devine D, Atema J. 1982. Function of chemoreceptor organs in spatial orientation of the lobster, *Homarus americanus*: differences and overlap. *Bio Bull*. 163:144–153.
- Felgenhauer B. 1992. External anatomy and integumentary structures of the Decapoda. In: Harrison F, Humes A, editors, *Microscopic Anatomy of Invertebrates*. New York: Wiley-Liss. p. 7–43.
- Fontaine M, Passelecq-Gerin E, Bauchau A. 1982. Structures chemoreceptrices des antennules du crabe *Carcinus maenas* (L.) (Decapoda Brachyura). *Crustaceana*. 43(3):271–283.
- Gaten E, Herring P, Shelton P, Johnson M. 1998. The development and evolution of the eyes of vent shrimps (Decapoda: Bresiliidae). *Cab Biol Mar*. 39:287–290.
- Gebruk A, Southward E, Kennedy H, Southward A. 2000. Food sources, behaviour, and distribution of hydrothermal vent shrimp at the Mid-Atlantic Ridge. *J Mar Biol Ass UK*. 80:485–499.
- Gleeson R, Carr W, Trapido-Rosenthal H. 1993. Morphological characteristics facilitating stimulus access and removal in the olfactory organ of the spiny lobster, *Panulirus argus*: insight from the design. *Chem Senses*. 18(1):67–75.
- Gleeson R, McDowell L, Aldrich H. 1996. Structure of the aesthetasc (olfactory) sensilla of the blue crab, *Callinectes sapidus*: transformations as a function of salinity. *Cell Tissue Res*. 284:279–288.
- Groh K, Vogel H, Stensmyr M, Grosse-Wilde E, Hansson B. 2014. The hermit crab's nose—antennal transcriptomics. *Front Neurosci*. 7:Article 266. doi:210.3389/fnins.2013.00266.
- Groh-Lunow K, Getahun M, Grosse-Wilde E, Hansson B. 2015. Expression of ionotropic receptors in terrestrial hermit crab's olfactory sensory neurons. *Front. Cell Neurosci*. 8:Article 448. doi:410.3389/fncel.2014.00448.
- Grünert U, Ache B. 1988. Ultrastructure of the aesthetasc (olfactory) sensilla of the spiny lobster, *Panulirus argus*. *Cell Tissue Res*. 251:95–103.
- Guenther C, Atema J. 1998. Distribution of setae on the *Homarus americanus* lateral antennular flagella. *Biol Bull*. 195:182–183.
- Guindon S, Dufayard JF, Lefort V, Anisimova M, Hordijk W, Gascuel O. 2010. New algorithms and methods to estimate maximum-likelihood phylogenies: assessing the performance of PhyML 3.0. *Syst Biol*. 59(3):307–321.
- Hallberg E, Johansson KU, Elofsson R. 1992. The aesthetasc concept: structural variations of putative olfactory receptor cell complexes in Crustacea. *Microsc Res Tech*. 22(4):325–335.
- Hallberg E, Skog M. 2011. Chemosensory sensilla in Crustaceans. In: Breithaupt T, Thiel M, editors, *Chemical communication in Crustaceans*. New York: Springer Science+ Business Media. p. 103–121.
- Herring P, Dixon DR. 1998. Extensive deep-sea dispersal of postlarval shrimp from a hydrothermal vent. *Deep-Sea Res I*. 45:2105–2118.
- Hoagland P, Beaulieu S, Tivey M, Eggert R, German C, Glowka L, Lin J. 2010. Deep-sea mining of seafloor massive sulfides. *Marine Policy*. 34(3):728–732.
- Hollins B, Hardin D, Gimelbrant AA, McClintock TS. 2003. Olfactory-enriched transcripts are cell-specific markers in the lobster olfactory organ. *J Comp Neurol*. 455(1):125–138.
- Husson B, Sarradin P, Zeppilli D, Sarrazin J. 2016. Picturing thermal niches and biomass of hydrothermal vent species. *Deep-sea Res. II*. In press. doi:http://doi.org/10.1016/j.dsr2.2016.05.028
- Jinks R, Battelle B, Herzog E, Kass L, Renninger G, Chamberlain S. 1998. Sensory adaptations in hydrothermal vent shrimps from the Mid-Atlantic Ridge. *Cab Biol Mar*. 39:309–312.
- Katoh K, Toh H. 2010. Parallelization of the MAFFT multiple sequence alignment program. *Bioinformatics*. 26(15):1899–1900.

- Keller T, Powell I, Weissburg M. 2003. Role of olfactory appendages in chemically mediated orientation of blue crabs. *Mar Ecol Prog Ser.* 261:217–231.
- Lahman SE, Moore PA. 2015. Olfactory sampling recovery following sublethal copper exposure in the rusty crayfish, *Orconectes rusticus*. *Bull Environ Contam Toxicol.* 95(4):441–446.
- Laverack MS. 1964. The antennular sense organs of *Panulirus argus*. *Comp Biochem Physiol.* 13:301–321.
- Le SQ, Gascuel O. 2008. An improved general amino acid replacement matrix. *Mol Biol Evol.* 25(7):1307–1320.
- Le Bris N, Govenar B, Le Gall C, Fisher C. 2006. Variability of physico-chemical conditions in 9 degrees 50' NEPR diffuse flow vent habitats. *Mar Chem.* 98(2–4):167–182.
- Letunic I, Bork P. 2011. Interactive Tree Of Life v2: online annotation and display of phylogenetic trees made easy. *Nucleic Acids Res.* 39:W475–W478.
- Machon J, Ravaux J, Zbinden M, Lucas P. 2016. New electroantennography method on a marine shrimp in water. *J Exp Biol.* 219(Pt 23):3696–3700.
- McCall JR, Mead KS. 2008. Structural and functional changes in regenerating antennules in the crayfish *Orconectes sanborni*. *Biol Bull.* 214(2):99–110.
- Mellon D Jr. 2012. Smelling, feeling, tasting and touching: behavioral and neural integration of antennular chemosensory and mechanosensory inputs in the crayfish. *J Exp Biol.* 215(Pt 13):2163–2172.
- Mellon D. 2014. Sensory Systems of Crustaceans. In: Derby C, Thiel M, editors, *The Natural History of the Crustacea. Vol. 3: Nervous Systems and Control Behavior*. New York: Oxford Univ. Press.
- Moore PA, Scholz N, Atema J. 1991. Chemical orientation of lobsters, *Homarus americanus*, in turbulent odor plumes. *J Chem Ecol.* 17(7):1293–1307.
- Pelli DG, Chamberlain SC. 1989. The visibility of 350 degrees C black-body radiation by the shrimp *Rimicaris exoculata* and man. *Nature.* 337(6206):460–461.
- Pond DW, Segonzac M, Bell MV, Dixon DR, Fallick AE, Sargent JR. 1997. Lipid and lipid carbon stable isotope composition of the hydrothermal vent shrimp *Mirocaris fortunata*: evidence for nutritional dependence on photosynthetically fixed carbon. *Mar Ecol Prog Ser.* 157:221–231.
- Ponsard J, Cambon-Bonavita MA, Zbinden M, Lepoint G, Joassin A, Corbari L, Shillito B, Durand L, Cuffe-Gauchard V, Compère P. 2013. Inorganic carbon fixation by chemosynthetic ectosymbionts and nutritional transfers to the hydrothermal vent host-shrimp *Rimicaris exoculata*. *ISME J.* 7(1):96–109.
- Renninger GH, Kass L, Gleeson RA, Van Dover CL, Battelle BA, Jinks RN, Herzog ED, Chamberlain SC. 1995. Sulfide as a chemical stimulus for deep-sea hydrothermal vent shrimp. *Biol Bull.* 189(2):69–76.
- Sandeman R, Sandeman D. 1996. Pre- and postembryonic development, growth and turnover of olfactory receptor neurones in crayfish antennules. *J Exp Biol.* 199(Pt 11):2409–2418.
- Sarradin P, Caprais J, Riso R, Kerouel R. 1999. Chemical environment of the hydrothermal mussel communities in the LuckyStrike and Menez Gwen vent fields, Mid Atlantic ridge. *Cab Biol Mar.* 40(1):93–104.
- Sarrazin J, Juniper K, Massoth G, Legendre P. 1999. Physical and chemical factors influencing species distributions on hydrothermal sulfide edifices of the Juan de Fuca Ridge, northeast Pacific. *Mar Ecol Prog Ser.* 190:89–112.
- Sarrazin J, Legendre P, De Brusserolles F, Fabri M, Guilini K, Ivanenko V, Morineaux M, Vanreusel A, Sarradin P. 2015. Biodiversity patterns, environmental drivers and indicator species on a High-temperature Hydrothermal edifice, mid-Atlantic ridge. *Deep-sea Res II.* 121:177–192.
- Schmidt M, Ache B. 1996a. Processing of antennular input in the brain of the spiny lobster, *Panulirus argus*. I. Non-olfactory chemosensory and mechanosensory pathway of the lateral and median antennular neuropils. *J Comp Physiol A.* 178:579–604.
- Schmidt M, Ache B. 1996b. Processing of antennular input in the brain of the spiny lobster, *Panulirus argus*. II. The olfactory pathway. *J Comp Physiol A.* 178:605–628.
- Schmidt M, Mellon D. 2011. Neuronal processing of chemical information in crustaceans. In: Breithaupt T, Thiel M, editors, *Chemical communication in Crustaceans*. New York: Springer Science+ Business Media. p. 123–147.
- Segonzac M. 1992. Les peuplements associés à l'hydrothermalisme océanique du Snake Pit (dorsale médio-Atlantique, 23°N, 3480m): composition et microdistribution de la mégafaune. *CR Acad Sci.* 314, série III:593–600.
- Segonzac M, de Saint-Laurent M, Casanova B. 1993. L'énigme du comportement trophique des crevettes Alvinocarididae des sites hydrothermaux de la dorsale médio-atlantique. *Cab Biol Mar.* 34:535–571.
- Shabani S, Kamio M, Derby CD. 2008. Spiny lobsters detect conspecific blood-borne alarm cues exclusively through olfactory sensilla. *J Exp Biol.* 211(Pt 16):2600–2608.
- Shillito B, Ravaux J, Sarrazin J, Zbinden M, Barthélémy D, Sarradin P. 2015. Long-term maintenance and public exhibition of deep-sea fauna: the AbyssBox Project. *Deep-Sea Res I.* 121:137–145.
- Stein L, Bao Z, Blasiar D, Blumenthal T, Brent M, Chen N, Chinwalla A, Clarke L, Clee C, Coghlan A, et al. 2003. The genome sequence of *Caenorhabditis briggsae*: a platform for comparative genomics. *PLoS Biol.* 1(2):e45. doi:10.1371/journal.pbio.0000045.
- Stepanyan R, Hollins B, Brock SE, McClintock TS. 2004. Primary culture of lobster (*Homarus americanus*) olfactory sensory neurons. *Chem Senses.* 29(3):179–187.
- Stuettgen P, Dudar O, Flavus T, Zhou M, Derby CD. 2001. Selective ablation of antennular sensilla on the Caribbean spiny lobster *Panulirus argus* suggests that dual antennular chemosensory pathways mediate odorant activation of searching and localization of food. *J Exp Biol.* 204(Pt 24):4259–4269.
- Tierney A, Thompson C, Dunham D. 1986. Fine structure of aesthetasc chemoreceptors in the crayfish *Orconectes propinquus*. *Can J Zool.* 64:392–399.
- The *C. elegans* Sequencing Consortium. 1998. Genome sequence of the nematode *C. elegans*: a platform for investigating biology. *Science.* 282(5396):2012–2018.
- Van Dover C, Fry B, Grassle J, Humphris S, Rona P. 1988. Feeding biology of the shrimp *Rimicaris exoculata* at hydrothermal vents on the Mid-Atlantic Ridge. *Mar Biol.* 98:209–216.
- Van Dover CL, Szuts EZ, Chamberlain SC, Cann JR. 1989. A novel eye in 'eyeless' shrimp from hydrothermal vents of the Mid-Atlantic Ridge. *Nature.* 337(6206):458–460.
- Vereshchaka AL, Kulagin DN, Lunina AA. 2015. Phylogeny and new classification of hydrothermal vent and seep shrimps of the family alvinocarididae (decapoda). *PLoS One.* 10(7):e0129975.
- Wharton D, Jinks R, Herzog E, Battelle B, Kass L, Renninger G, Chamberlain S. 1997. Morphology of the eye of the hydrothermal vent shrimp *Alvinocaris markensis*. *J Mar Biol Ass UK.* 77:1097–1108.
- Zbinden M, Le Bris N, Gaill F, Compère P. 2004. Distribution of bacteria and associated minerals in the gill chamber of the vent shrimp *Rimicaris exoculata* and related biogeochemical processes. *Mar Ecol Prog Ser.* 284:237–251.
- Zbinden M, Shillito B, Le Bris N, De Vilardi de Montlaur C, Roussel E, Guyot F, Gaill F, Cambon-Bonavita M-A. 2008. New insights on the metabolic diversity among the epibiotic microbial community of the hydrothermal shrimp *Rimicaris exoculata*. *J Exp Mar Biol Ecol.* 159(2):131–140.
- Zhang D, Cai S, Liu H, Lin J. 2008. Antennal sensilla in the genus *Lysmata* (Caridea). *J Crust Biol.* 28(3):433–438.